

iPSC-hepatocyte organoids as a novel platform to predict AAV gene therapy efficacy

Estelle Berreur,¹ Giacomo Lazzaroni,¹ Cyrill Roth,² Marco Zihlmann,¹ Martina Stirn,¹ Ramona Matheis,¹ Rebecca Xicluna,¹ Ekaterina Breous-Nyström,¹ and Adrian B. Roth³

¹Roche Pharma Research and Early Development, Roche Innovation Center Basel, CH-4070 Basel, Switzerland; ²Institute of Human Biology, Roche Innovation Center Basel, CH-4070 Basel, Switzerland; ³Precision Safety, Pharma Product Development, Roche Innovation Center Basel, CH-4070 Basel, Switzerland

Adeno-associated virus (AAV) vectors are widely used in gene therapy, particularly for liver-targeted treatments. However, predicting human-specific outcomes, such as transduction efficiency and hepatotoxicity, remains challenging. Reliable *in vitro* models are urgently needed to bridge the gap between preclinical studies and clinical applications. This study presents the first comparative evaluation of AAV transduction across multiple induced pluripotent stem cell (iPSC)-derived hepatocyte organoid donors, offering a novel platform for assessing vector performance in human liver models. The transduction efficiency and hepatotoxicity of eight AAV serotypes (AAV1, AAV2, AAV3, AAV4, AAV5, AAV6, AAV8, and AAV9) were tested in iPSC-derived liver organoids and hepatic cell lines (HepG2 and HepaRG). AAV6 and AAV8 exhibited the highest transduction efficiency in organoids, while AAV4 and AAV5 were the least effective. Transduction variability was observed across different donors and cell lines. Notably, no significant hepatotoxicity, measured by AST (aspartate aminotransferase) release and viability measurements, was observed, indicating that AAVs do not induce immediate liver damage *in vitro*. This study introduces iPSC-derived hepatocyte organoids as a novel and effective tool for predicting AAV transduction efficiency and safety, with potential to enhance the translation of gene therapies to clinical applications.

INTRODUCTION

Recombinant adeno-associated viral vectors (rAAVs) have become the main gene delivery method for *in vivo* gene therapy applications. In 2012, Glybera was authorized by the European Medicines Agency (EMA) as the first human gene therapy for the treatment of acute pancreatitis in patients with lipoprotein lipase deficiency, a rare hereditary lipid disease.¹ To date, seven gene therapy products based on AAV vectors are authorized on the market: Luxturna (RPE65 mutation-associated retinal dystrophy, based on AAV2),² Zolgensma (pediatric patients with spinal muscular atrophy, based on AAV9),³ Hemgenix (hemophilia B, based on AAV5),⁴ Elevidys (Duchenne muscular dystrophy, based on AAVrh74),⁵ Roctavian (hemophilia A, based on AAV5),⁶ Upstaza (aromatic L-amino acid decarboxylase deficiency, based on AAV2),⁷ and Beqvez (hemophilia B, based on AAVrh74var).⁸ In addition, there are more than 366 adeno-associ-

ated virus (AAV)-based gene therapy clinical trials ongoing (based on Gene Therapy Clinical Trials Worldwide database, November 2024).⁹

Due to its role in human metabolism and some other important physiologic activities such as digestion, immunity, blood clotting, or protein synthesis,^{10,11} the liver has been one of the first target organs for systemic administration of AAV-mediated gene therapy. First liver targeting gene therapy studies were conducted in the context of hemophilia A and B. In both mice and humans, a recombinant AAV2 vector expressing human factor IX (hFIX) demonstrated efficiency for hemophilia B by inducing stable, therapeutic levels of factor IX in plasma after a single infusion.^{12,13} Building on these promising results, years of extensive research and advancements in AAV vector design eventually led to the approval in 2022 of the first liver-directed gene therapy product, utilizing an AAV5 vector with a liver-specific promoter, for the treatment of hemophilia B.

Studies on hemophilia B have revealed notable distinctions in the responses to AAV-mediated gene therapy between preclinical animal models and humans. The first clinical trials demonstrated a transient expression of the transgene product and liver toxicity in some patients, including activation of capsid-specific T cells and direct hepatocellular damage.^{14,15} Interestingly, these issues were absent in small animal models, as well as non-human primate models. However, liver toxicity in humans is not solely limited to T cell responses. Other forms of hepatotoxicity linked to the overexpression of the transgene disrupting the normal metabolism of the cells have been reported in animals, as well as acute hepatocellular injury that occurs within the first 3 to 10 days after vector administration.^{16–19} For instance, a study using a self-complementary AAV8 vector encoding a codon-optimized hFIX (AAV2/8-LP1-hFIXco) initially showed promising results in 24 non-human primates, with stable transgene expression and no toxicity.²⁰

Received 20 December 2024; accepted 9 April 2025;
<https://doi.org/10.1016/j.omtm.2025.101467>

Correspondence: Estelle Berreur, Roche Pharma Research and Early Development, Roche Innovation Center Basel, Grenzacherstrasse 124, CH-4070 Basel, Switzerland.

E-mail: estelle.berreur@roche.com



When administered to six patients, although the vector exhibited efficiency with long-term hFIX expression, it also led to elevated serum liver enzymes in two of them who received the highest dose, potentially being the consequence of a cellular immune response to the AAV capsid.²¹

Furthermore, AAV-mediated therapies not targeting the liver can also induce liver toxicity, as most AAV serotypes exhibit a strong natural tropism for this organ. Animal studies have revealed that AAV liver tropism varies across species.^{22–24} Another study confirmed species differences in the transduction efficiency of several AAV serotypes in murine, hamster, and monkey immortalized cell lines.²⁵ Therefore, there is significant lack of translatability between animal models and humans, highlighting the urgent need for better models to predict the liver transduction by different AAVs as well as the safety risk in case of viral uptake of the virus by the liver even if it is not the targeted organ.

In the pursuit of applying preclinical findings to humans in the context of AAV, the intricate challenge of tissue-tropism differences between species is compounded by the complex interplay of the T cells' differentiation status and functionality, pre-existing immunity, and biodistribution, contributing to the complexity of interpreting research outcomes.^{26,27} Utilizing a human cell system can aid in understanding these differences. However, the introduction of patient-to-patient variability further complicates the analysis of clinical data, making it challenging to draw conclusions about the performance of individual vectors. Thus, a reliable *in vitro* system for testing AAV toxicity in the liver has not been available.

Aiming to close this critical gap, we assessed in the present study the transduction efficiency of various AAV serotypes (AAV1, AAV2, AAV3, AAV4, AAV5, AAV6, AAV8, and AAV9) in a variety of *in vitro* human liver models, including hepatic cell lines (HepG2 and HepaRG) and induced pluripotent stem cell (iPSC)-derived liver organoids. We then assessed direct hepatotoxicity by measuring liver transaminases and viability of the system after treatment. This work demonstrates the potential of liver organoids to serve as an efficient tool to model AAV transduction. It also contributes toward a better understanding of whether *in vitro* models such as liver organoids can serve as a platform for *in vivo* prediction of AAV hepatotoxicity.

RESULTS

HepG2 and HepaRG are both transduced by AAV 2, 3, 4, 5, 6, 8, and 9

The most widely known human liver model relies on hepatocyte cell lines. In this regard, HepG2 and HepaRG were initially utilized to assess AAV transduction efficiency using AAV2, 3, 4, 5, 6, 8, and 9. Cells were exposed to AAVs encoding GFP (green fluorescent protein) as reporter transgene at a multiplicity of infection (MOI) of 10^6 , and GFP expression was analyzed over 3 days. A preliminary experiment using AAVs at MOI of 10^4 , 10^5 , and 10^6 demonstrated the highest transduction at an MOI of 10^6 (data not shown). First, initiation of GFP expression was observed approximately 4–8 h post-

treatment (Figures 1A and 1B). The transduction efficiencies varied according to the AAV serotypes in both cell lines (Figure 1A). Interestingly, HepG2 cells exhibited superior transduction by AAV2 compared to other serotypes, whereas AAV8 and AAV9 displayed lower transduction rates. In contrast, HepaRG cells demonstrated highest transduction with AAV6, while AAV2, 8, and 9 showed relatively similar transduction efficiency (Figure 1B). Overall, all tested serotypes achieved transduction efficiencies exceeding 50% in HepaRG cells. In HepG2, AAV2, 3, and 6 showed the highest transduction efficiency (68.80%, 69.25%, and 54.45%, respectively), whereas AAV8 and AAV9 were poorly transduced (13.74% and 25.03%, respectively) (Figure 1C). These findings underscore the substantial impact of AAV serotypes and model selection to study AAV transduction.

iPSC-derived hepatocytes form 3D organoids

As primary hepatocytes are known to be difficult to transduce by AAVs,²⁵ we decided to use iPSC-derived hepatocytes in order to have an *in vitro* model that could potentially recapitulate inter-donor variability. To generate the iPSC-derived hepatocyte organoid liver model, we first optimized the culture conditions to ensure reproducibility. Our approach, utilizing iPSC-derived hepatocyte organoids, involved the encapsulation of single cells within Matrigel, yielding the formation of multiple organoids per well as shown in Figure 2A. Different cell concentrations were tested to identify the most effective conditions for organoid formation following a 14-day differentiation period. Notably, we observed the development of 2D structures at the bottom of the wells, which we considered cells adhering to the plastic and failing to aggregate into 3D structures. To overcome this problem, we applied coating with Matrigel of the wells prior to cell seeding, which effectively prevented formation of 2D structures, yielding more reproducible organoid structures (Figure S1).

We observed that hepatocytes were forming interconnections and self-organized by day 2 (Figure 2B). On day 7 and day 14, organoids were clearly detectable. To monitor hepatocyte differentiation throughout the culture period, we assessed the expression of specific genes associated with hepatocytes and stem cells by reverse transcription quantitative PCR (RT-qPCR). As expected, the expression of albumin (*ALB*) and alpha-1-antitrypsin (*AAT*; gene symbol *SERPINA1*) gradually increased during maturation before plateauing after day 14 (Figure 2C). Asialoglycoprotein receptor 1 (*ASGR1*) and asialoglycoprotein receptor 2 (*ASGR2*), receptors located at the surface of the hepatocytes, showed stable expression in pre-differentiated hepatocytes at the outset of the culture. Concurrently, fetal hepatocyte markers alpha-fetoprotein (*AFP*) and leucine-rich repeat-containing G-protein-coupled receptor 6 (*LGR6*) displayed reduced expression with increasing culture time. To confirm these findings at the protein level, immunofluorescence staining was done after 14 days of culture (Figure 2D). Notable expression of key hepatocytes markers, *ALB*, *AAT*, and *ASGR1*, was observed affirming the differentiation into hepatocytes (Figure 2D). These results indicate successful establishment of

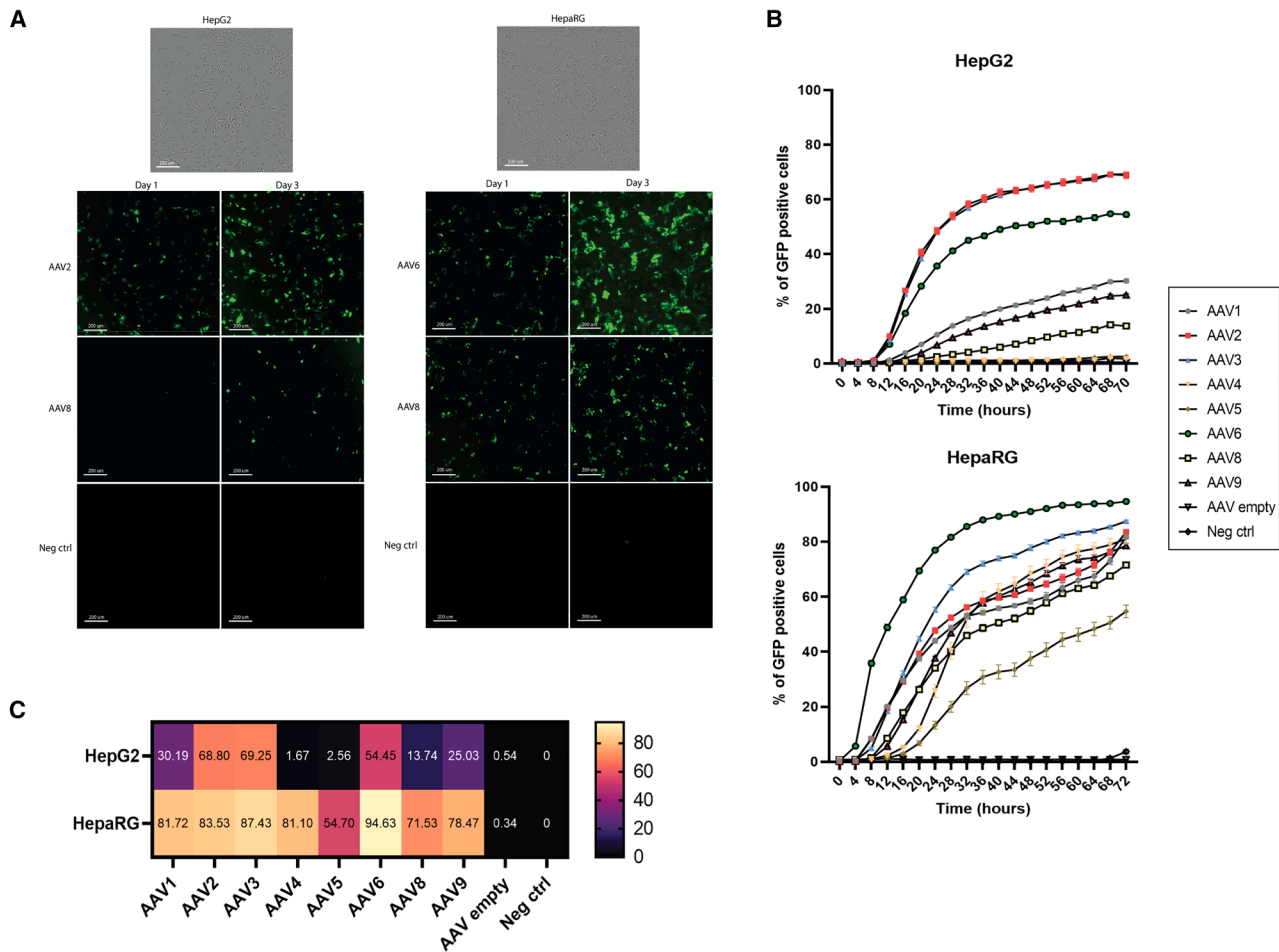


Figure 1. Analysis of AAV transduction in cell lines

(A) Phase-contrast and immunofluorescence images of AAV2 and AAV8 transduction in HepG2 and AAV6 and AAV8 transduction in HepaRG cell lines at day 1 and day 3. Scale bar, 200 μ m. (B) AAV transduction efficiency overtime in percentage for HepG2 or HepaRG during 3 days. Data are expressed as mean (SD) ($n = 3$). (C) Heatmap representing the mean of the percentage of AAV-transduced cells 3 days after AAV treatment, for HepG2 and HepaRG.

culture conditions allowing the generation of iPSC-derived hepatocyte organoids.

iPSC-derived hepatocyte organoids are transduced by various AAV serotypes and show donor variability

To verify if the iPSC-derived hepatocyte organoids could serve as AAV transduction models, first, AAV8 and AAV9 were tested at MOI 10^4 , 10^5 , and 10^6 in two donors. As expected, the number of GFP-positive organoids was observed to be AAV dose-dependent, with the highest percentage of GFP-positive organoids obtained with an MOI of 10^6 for both AAV8 and AAV9 in donors 1 and 2 (Figure 3A).

Then, iPSC-derived hepatocytes organoids were exposed to AAV2, 3, 4, 5, 6, 8, and 9 at 10^6 MOI. GFP expression was analyzed up to 4 weeks. On day 2 after treatment with AAVs at a 10^6 MOI, no clear GFP signal could be detected for any of the serotypes, indicating the

requirement of an initiation period for transduction and GFP expression as shown for AAV5 and 8 on Figure 3B. From day 14 onward, the GFP signal was clearly visible.

After an initial lagging phase, the GFP expression rapidly reached a plateau (approximately 7 days post-transduction) (Figure 3C). Moreover, the GFP signal remained constant until day 28, indicating prolonged expression in organoids.

As expected, donor heterogeneity was observed, with donor 3 showing approximately 50% lower transduction efficiency across all tested serotypes. Furthermore, variability in transduction efficiency was evident among serotypes within different donors. Despite the donor heterogeneity, the trend in serotype transduction efficacy was consistent across donors. For instance, while AAV8 and AAV9 demonstrated superior transduction in donor 1, AAV6 surpassed other serotypes in donors 2, 3, and 4

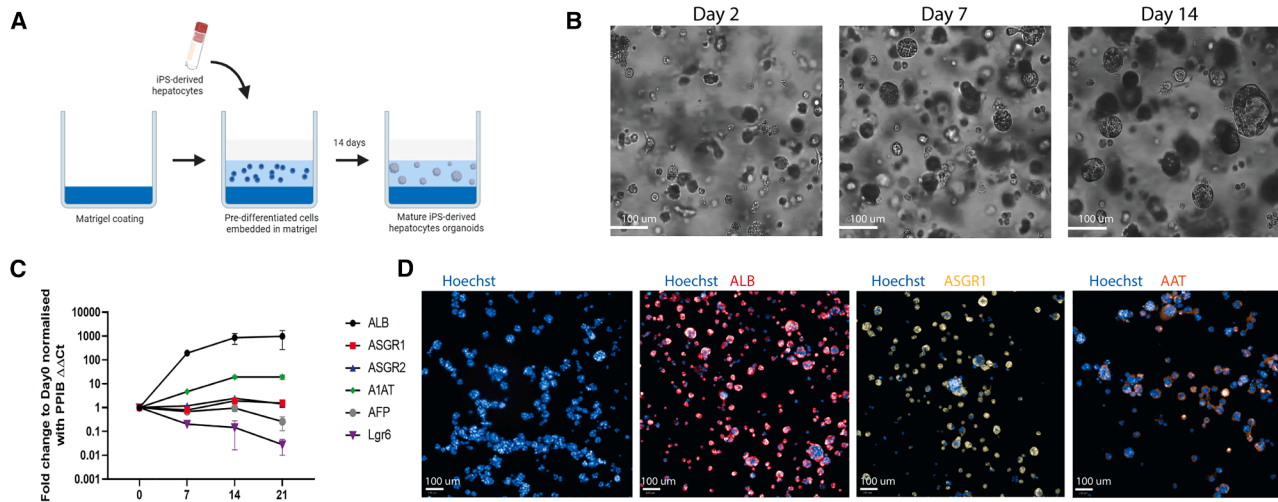


Figure 2. Establishment and characterization of the iPSC-derived 3D hepatocytes model

(A) Schematic overview of the culture protocol. (B) Phase-contrast images of the culture. Scale bar, 100 μ m. (C) RT-qPCR analysis of genes associated with hepatocytes (*ALB*, *ASGR1*, *ASGR2*, and *A1AT*), fetal hepatocytes (*AFP*), and stem cells (*Lgr6*). Data are expressed as mean (SD) ($n = 3$, normalized to PPIB). (D) Immunofluorescence images of hepatocytes markers (*ALB*, *ASGR1*, and *AAT*). Scale bar, 100 μ m.

(Figures 3C and 3D). Overall, every AAV serotype tested successfully transduced iPSC-derived hepatocyte organoids from all four donors, with AAV4 and AAV5 displaying the lowest transduction efficiency (average among the four donors of 15.23% and 12.94%, respectively) and AAV2, 6, 8, and 9 showing the highest efficiency (average among the four donors of 39.62%, 55%, 40.52%, and 41.49%, respectively) (Figure 3D). These results underline the significant role of AAV serotypes, donor variability, and viral dose for the transduction efficiency of iPSC-derived hepatocyte organoids.

AAVs did not induce direct hepatocellular damage

To determine if those different models could allow evaluation of AAV-hepatotoxicity, we assessed aspartate aminotransferase (AST) levels in the different models 2 days post-treatment with different conditions. HepG2, HepaRG, and the four organoid donors showed a substantial increase in AST levels following treatment with adenovirus or chlorpromazine when compared to their respective controls (Figure 4A). Adenovirus and chlorpromazine both can be used as positive controls for liver toxicity, as adenovirus induces liver damage through viral replication and immune responses,²⁸ while chlorpromazine causes hepatotoxicity via oxidative stress and mitochondrial dysfunction.^{29,30} These observations highlighted that these models can recapitulate direct hepatotoxicity.

Notably, incubation with AAV2, AAV8, and AAV9 did not yield a significant increase in AST levels at day 2 either in cell lines or in organoid cultures. These findings collectively suggest that within this initial phase post-treatment, these AAV serotypes do not induce AST-related acute liver damage in the liver models under investigation.

As organoids could be maintained in culture for extended periods compared to cell lines, more prolonged assessment of AST release post-treatment was conducted (up to 28 days post-treatment). In line with previous observations, Figure 4B illustrates AST release 2 days after treatment with adenovirus and chlorpromazine. While the timing of AST release was consistent across donors, the levels detected were highly variable (between 2 and 10 U/mL). This highlights donor-specific responses to these hepatotoxic agents. Conversely, over the 28-day culture period, no significant escalation of AST release was noted following treatment with various AAV serotypes. This sustained absence of AST release confirmed the reduced risk for direct hepatotoxicity with the administered AAVs in this specific model and time frame.

In parallel with AST measurements, viability of the systems was tested by measurement of adenosine triphosphate (ATP) levels 72 h post-treatment of HepG2 and HepaRG and 28 days post-treatment for the organoids. Figure 4C shows a high decrease of ATP following chlorpromazine treatment, indicating cell death, on both HepG2 and HepaRG cells. In correlation with previous results, no significant decrease of ATP was observed following AAV treatments. Similar results were found on the organoids 28 days after treatment (Figure 4D).

DISCUSSION

Despite the progress made with recombinant AAV vectors, the precise biodistribution, dissemination, toxicity, and duration of transgene expression of these vectors in the human body following administration is not fully understood.³¹ There have also been notable differences between outcomes in preclinical studies including NHPs and human trials, resulting in patients unable to experience full benefits of the therapy.

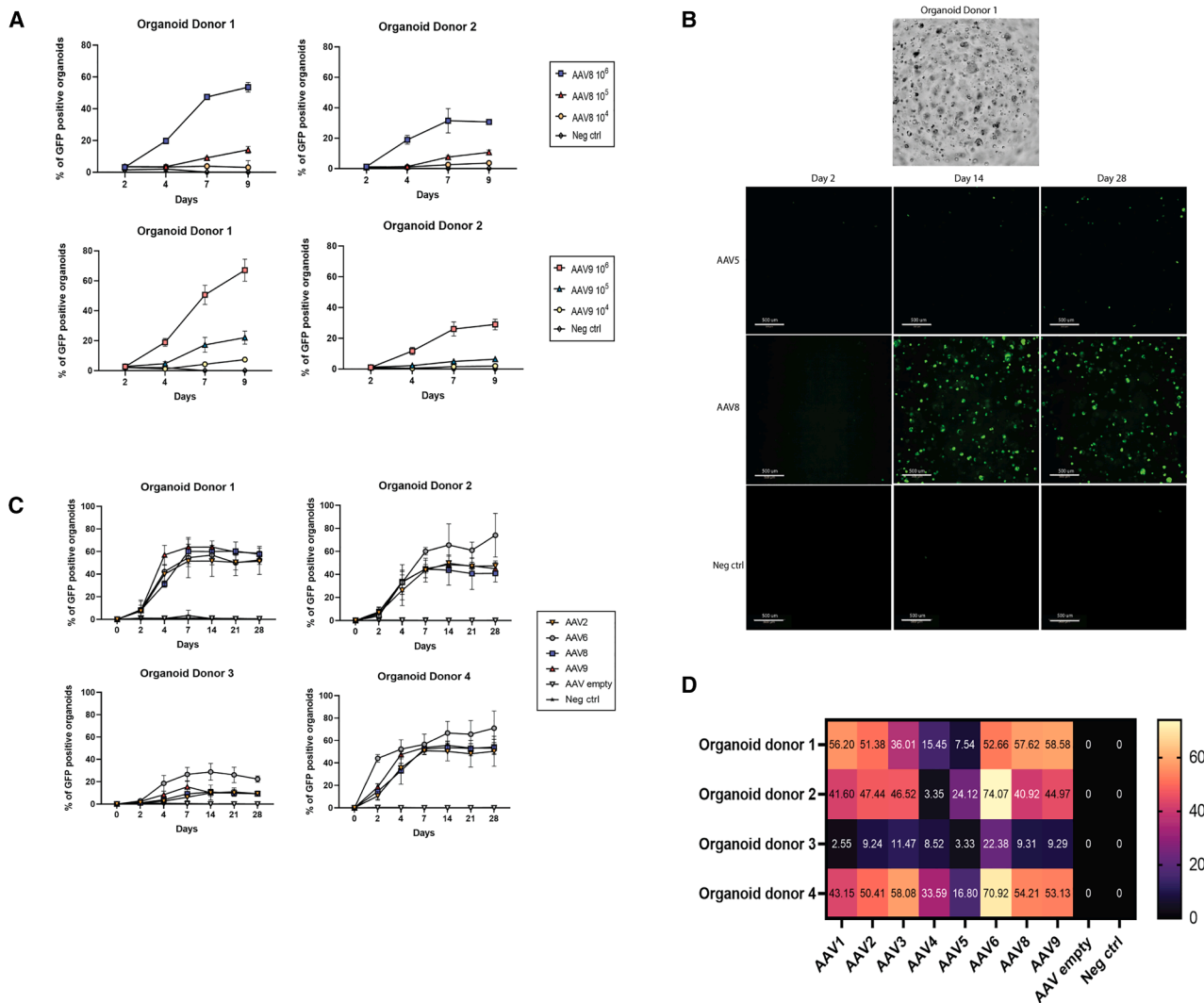


Figure 3. Analysis of the AAV transduction in iPSC-derived hepatocyte organoids

(A) AAV transduction efficiency with different concentrations (MOI 10⁴, 10⁵, and 10⁶) for donor one and two for 9 days. Data are expressed as mean (SD) (n = 3). (B) Phase-contrast and immunofluorescence images of AAV5 and AAV8 (MOI 10⁵) transduction iPSC-derived hepatocyte organoids at day 2, day 14, and day 28. Scale bar, 500 μm. (C) AAV transduction efficiency at a 10⁶ MOI overtime in percentage for the organoids (4 donors) for 28 days. Data are expressed as mean (SD) (n = 3). (D) Heatmap representing the mean of the percentage of GFP-positive organoids 28 days after AAV treatment (MOI 10⁶) for the four-organoid donors for AAV1 to AAV9.

Preclinical liver models, ranging from immortalized hepatocyte cell lines, like HepG2, to animal models such as mice and other rodents, humanized mouse models, non-human primates, organoids, and tissue slice cultures, have been extensively utilized for evaluating the transduction efficiency and toxicity of AAV vectors. In this study, we compared the transduction efficiencies in human-relevant models, employing HepG2 and HepaRG cell lines, along with iPSC-derived hepatocyte organoids obtained from four distinct donors, for eight AAV serotypes: AAV1, 2, 3, 4, 5, 6, 8, and 9.

The most widely known human liver model relies on hepatocyte cell lines. HepG2, derived from hepatocellular carcinoma, repre-

sents an immortalized cell line capable of self-renewal, widely accessible for cost-effective experiments. Also derived from hepatocellular carcinoma, HepaRG cells exhibit greater differentiation into mature hepatocyte-like cells compared to HepG2 but are more expensive due to their proprietary nature. Our results demonstrated significant differences in the transduction efficiency of various AAV serotypes between the two immortalized hepatocyte cell lines. Consistent with previous findings, AAV2, 3, and 6 transduced HepG2 cells more effectively than AAV1, 4, 5, 8, and 9.³² In contrast, all tested serotypes (AAV1, 2, 3, 4, 5, 6, 8, and 9) exhibited high transduction efficiency in HepaRG cells. The limited transduction observed in HepG2 cells for certain

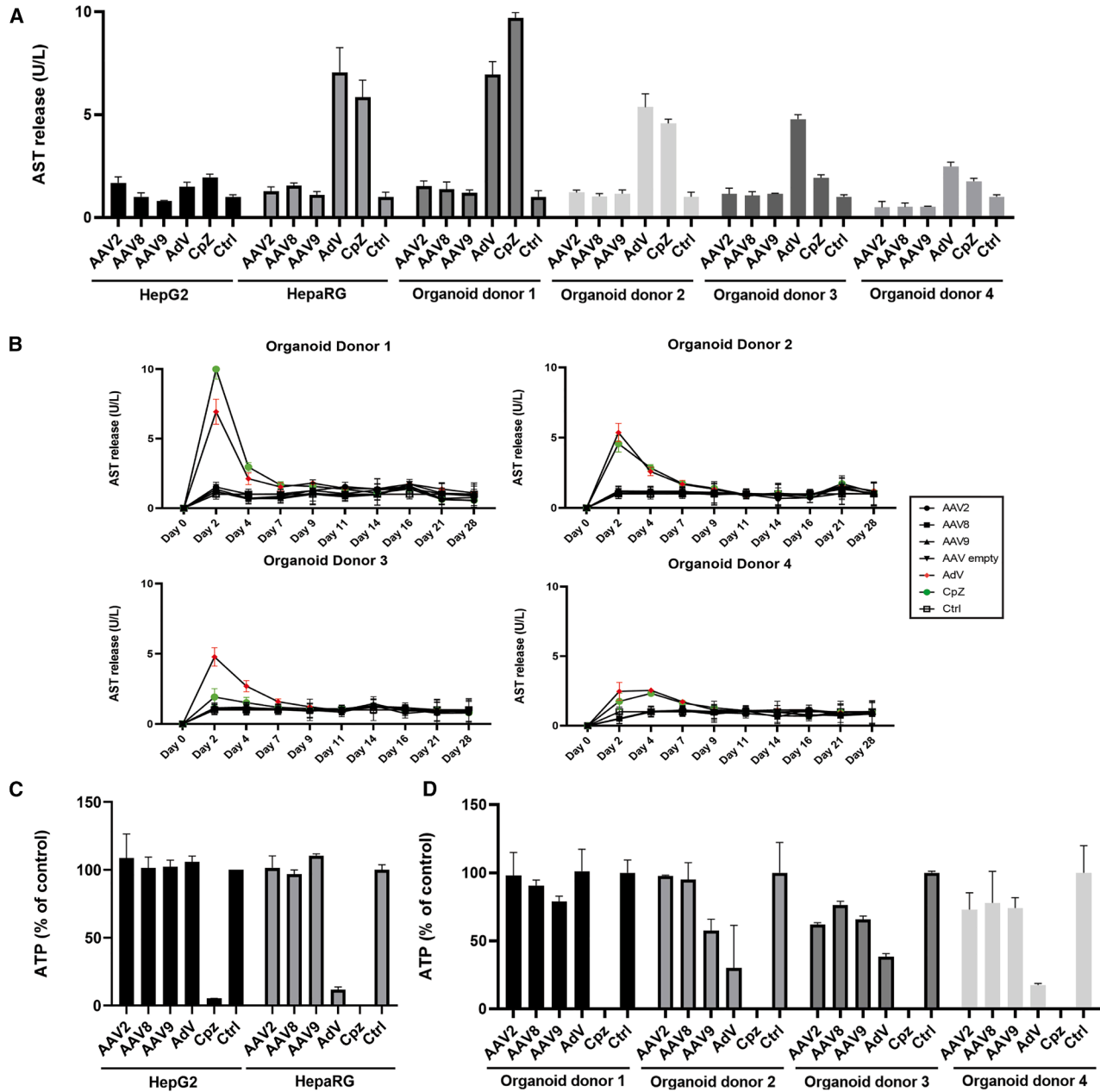


Figure 4. Evaluation of toxicity on the different models

(A) AST release 2 days post-treatment on HepG2, HepaRG, and iPSC-derived organoids. The results were normalized to the respective negative control for each liver model. Data are expressed as mean (SD) ($n = 3$). (B) AST release in the supernatant of four donor-derived organoids up to 28 days post-AAV-transduction. The results were normalized to the donor-matched negative control. Data are expressed as mean (SD) ($n = 3$). (C) ATP content on HepG2 and HepaRG 72 h after treatments. Data represented in %, with 100% being the reference value of the negative control \pm standard deviation ($n = 3$). (D) ATP content on organoids 28 days after treatments. Data represented in %, with 100% being the reference value of the negative control \pm standard deviation ($n = 3$).

serotypes may not fully reflect viral performance in clinical contexts. For instance, AAV8 and AAV5, known for their strong liver tropism *in vivo*, has been successfully used in patients with severe hemophilia B, where it enabled long-term expression of therapeutic factor IX. The more efficient transduction of HepaRG than

HepG2 by AAV8 and AAV5 shown as efficient in clinical trials^{6,8,13} suggests that HepaRG cells may be a better model to recapitulate the transduction clinical outcomes. However, the performance of AAV variants in HepaRG cells has been less frequently explored.

We attempted to transduce primary liver spheroids with various AAV serotypes, which resulted in limited viral uptake (data not shown). In contrast, using iPSC-derived hepatocyte organoids, we observed effective transduction with several AAV serotypes. This difference could be attributed to the more accessible cellular architecture of iPSC-derived models, which better mimic certain functional aspects of hepatocytes. Primary liver spheroids, although physiologically relevant, often present barriers such as limited permeability or more complex extracellular matrix structures that may hinder AAV transduction.

iPSC-derived hepatocyte organoids have emerged as a promising tool to better understand liver-specific functions, develop new therapeutic approaches, and improve the efficiency of screening for potential drug candidates. In addition, iPSCs represent an immortal source of cells that can be derived from patient samples with specific genetic backgrounds and diseases, allowing studies on disease mechanisms and personalized drug responses. In the gene therapy field, iPSC-derived hepatocytes have the potential to offer a valuable platform for investigating both the safety and efficacy of AAV-mediated gene therapy products. In our study, we assessed AAV transduction efficiency across four distinct donors. Despite the donor variability, the consistent trend in efficacy was observed across donors. AAV4 and 5 were less efficient to transduce when compared to AAV1, 2, 6, 8, or 9. Notably, AAV2, 8, and 9 are known to well transduce the liver in humans. Although AAV5 is used in approved liver-targeted gene therapies, its lower efficiency in our study is somewhat surprising.

Research indicates that the efficiency of AAV transduction can be influenced by several factors, which may explain the discrepancy we observed between the different models. One key factor is the expression level of the AAV receptors and co-receptors in these models. AAV receptor (AAVR, also known as KIAA0319L) is one of the primary receptors for various AAV serotypes; studies have shown that cells with higher AAVR expression tend to exhibit increased AAV uptake and transduction efficiency.³³ Heparan sulfate proteoglycans (HSPGs) also serve as key initial binding sites for some AAV serotypes, notably AAV2.³⁴ Further studies have identified other primary receptors critical for the transduction of different AAV serotypes.^{35,36} In addition to primary receptors, AAV co-receptors significantly enhance transduction efficiency.^{37,38} Variations in AAV transduction efficiency among the iPSC-derived hepatocyte organoid donors, as well as the differences observed in the two immortalized cell lines, may be attributed to differences in the expression of AAV receptors and co-receptors. These variations warrant further in-depth study of the expression of these different receptors in the different models. It is also important to note that the liver models tested included only hepatocytes. The liver is a complex organ composed of various cell types, including Kupffer cells, stellate cells, and liver sinusoidal endothelial cells, which might also impact the transduction of the various serotypes. Finally, it is important to note that following systemic delivery, AAV distribution is broad, and several organs can uptake the vector, with varying affinity de-

pending on the serotype, thereby impacting the amount of AAV reaching the liver. To better account for this parameter, human chimeric mouse models, such as the xenografted FRG mouse model or the PiZ-NSG mouse model, might provide more relevant insights.

One of the main concerns associated with AAV-driven gene therapy, particularly when looking at the liver, is the potential for inducing toxicity. Liver transaminases, such as AST, are enzymes typically found in the liver. Elevated levels of these enzymes in the bloodstream serve as clinical markers of liver damage and have been reported in multiple gene therapy clinical studies.³⁹ Therefore, to assess the impact of AAV treatment on AST production, we investigated its effects on the two immortalized cell lines and the four iPSC-derived hepatocyte organoid donors. Our findings revealed that AAV transduction did not lead to a significant increase in AST levels, indicating an absence of hepatocellular damage in these models. This suggests that, under the conditions tested, AAV vectors did not induce liver toxicity. On the contrary, chlorpromazine and adenovirus were used as positive controls for liver toxicity induction and showed signs of liver transaminase increase. Their toxicity mechanism involves direct hepatocyte damage, which leads to the release of liver enzymes like AST into the bloodstream or culture supernatant, making it detectable in our assessments. Viability measurements were consistent with AST release. As mentioned previously, the liver is composed of several cell types, each playing a crucial role in liver function and response to injury. Kupffer cells, for instance, are liver-resident macrophages that are key players in the immune response and can significantly influence the outcome of AAV transduction through their ability to trigger inflammatory responses.⁴⁰ Stellate cells are involved in liver fibrosis, whereas sinusoidal endothelial cells contribute to the vascular environment of the liver. The absence of these cell types in our *in vitro* models may limit the ability to fully predict the potential hepatotoxic effects of AAV vectors *in vivo*. In addition, the models presented in this study do not include immune effector cells, which may play a crucial role in the liver toxicity observed in AAV-mediated gene therapy. To address this, incorporating peripheral blood mononuclear cells into the model or utilizing a vascularized liver model with blood flow would be of interest for further investigation. Therefore, future studies should include more comprehensive liver models incorporating these various cell types to better understand the interactions and potential toxicities that may arise during AAV-mediated gene therapy in a more physiologically relevant context. Such model can be achieved with iPSC as they can be differentiated in several cell types from the same donor.

In conclusion, our study demonstrates a robust and effective transduction of various hepatocyte-based models *in vitro* by recombinant AAV vectors, although discrepancies in transduction efficiency were observed. This study underscores the importance of thoroughly characterizing and assessing *in vitro* models for their translatability. Selecting the appropriate model is crucial, depending on the specific research question being addressed. Our findings provide valuable insight into choosing the most relevant model to answer specific

questions related to AAV transduction efficiency and potential therapeutic applications.

MATERIALS AND METHODS

Cell culture

HepG2 cells were thawed at 37°C for 3 min. Cells were transferred to a 15 mL falcon tube containing 9 mL of MEM (minimum essential medium, Gibco, 41090) with 10% FBS (fetal bovine serum; Gibco 16140071). Cells were counted, centrifuged at 125 g for 5 min at room temperature (RT), and resuspended in culture medium at the desired concentration. Cells were seeded in a collagen-type-I-coated flask (Corning, 356484) and cultured for two passages.

NoSpin HepaRG cells (BioPredic International, HPR116NS) were thawed according to manufacturer's instructions. Briefly, cells were thawed at 37°C for 3 min. Cells were resuspended to a volume of thawing and plating media (Lonza, MHTAP) provided by the certificate of analysis. Then, 100 µL of the cell suspension was seeded to a Costar 96-well BioCoat plate (Corning, 354407). On day 1, 24 h after seeding, the media was changed to the maintenance media (Lonza, MHMET). The media was replaced on days 4 and 6.

Culture iPSC-derived hepatocyte organoids

Human iPSC-derived cells used in this study were obtained from DefiniGEN (Cambridge, UK), a commercial provider. The cells were supplied in an anonymized, de-identified format, and therefore, use of these materials does not require oversight by an Institutional Review Board, in accordance with institutional and international ethical guidelines. Wild-type iPSC-derived hepatocytes from four different donors were sourced from DefiniGEN. Pre-differentiated cryopreserved cells were delivered at 4–6 million viable cells per vial and consist of 99% hepatocytes according to the vendor. DefiniGEN thawing and plating medium (DTM), as well as DefiniGEN recovery and maintenance medium (DRM) were prepared according to manufacturer's instructions. A 96-well flat bottom plate (Corning, 3904) was coated with 30 µL Matrigel (Corning, 356231) and incubated for 30 min at 37°C. Cells were thawed at 37°C for 3 min, transferred into 10 mL DTM, mixed, and counted. Cells were centrifuged at RT for 5 min at 100 g, the supernatant was removed, and the cells were resuspended in DRM containing 1 µL/mL of ROCK inhibitor (Selleckchem, S1049) to the desired concentration to plate 80,000 cells per well. A 2:1 Matrigel:cell suspension was prepared, and 60 µL of the mix was seeded in the plate. After 1 h of incubation at 37°C and 5% CO₂, 100 µL of DRM was added to each well, and the plate was placed in the incubator. Media exchange was performed every 2–3 days, and Matrigel was added on top weekly with 66 µL of Matrigel in 1 mL of DRM during media exchange.

Treatments

AAV constructs produced in Sf9 cells through infection with two recombinant baculoviruses were sourced from Virovek: AAV1, AAV2, AAV3, AAV4, AAV5, AAV6, AAV8, and AAV9 expressing green fluorescent protein (GFP) and empty AAV2, AAV8, and AAV9

were used under a cytomegalovirus (CMV) promoter. Constructs were purified by two rounds of cesium chloride ultracentrifugations.

Upon reaching approximately 80% confluence, HepG2 cells were detached and seeded at 15,000 cells per well in a Costar 96-well BioCoat plate (Corning, 4407). After 6 h of incubation to let the cells adhere, the media was removed, and the cells were subjected to an AAV/deferioxamine (DFO) cocktail consisting of 100 µL per well of MEM (Gibco, 41090) with 10% FBS (Gibco 16140071), with 100 µM DFO (Sigma, 9533) to stop the proliferation of the cells and AAVs to a 10⁶ multiplicity of infection (MOI: ratio of virus to target cells). Transduction was followed by imaging for 3 days using the Incucyte S3 (Sartorius, 4647).

After 7 days of culture, media of NoSpin HepaRG was removed, and the cells were exposed with 100 µL of HepaRG maintenance media containing AAVs (MOI 10⁶). Transduction was followed by imaging for 3 days using the Incucyte S3 (Sartorius, 4647).

After 14 days of differentiation, organoid culture medium was replaced by 100 µL of fresh media containing AAVs (MOI 10⁶). Transduction was followed by imaging for 28 days using Opera Phenix high-content screening system (PerkinElmer).

The transduction efficiency was calculated as a percentage of GFP-positive cells over the total number of cells.

As controls and tox inducers, cells were treated with 150 µM chlorpromazine (Sigma, C8138) or AdV (VectorBuilder, AVF35M (VB200401-6014bgr)) to a 10³ MOI.

RT-qPCR

Total RNA extraction was performed using the RNeasy Micro Kit (QIAGEN, 74004), and 300 ng RNA was transcribed into complementary DNA (cDNA) using the QuantiTect Reverse Transcription Kit (QIAGEN, 205311) according to manufacturer's instructions. Amplification cycles were performed on QuantStudio 7 Flex Real-Time PCR System, 384-well (Thermo Fisher Scientific, 4485701) using TaqMan Gene Expression Assays (Applied Biosystems, 4331182; 4448489) and TaqMan Fast Advanced MasterMix (Applied Biosystems, 4444556).

Primers included *ALB* (Hs00609411_m1), *ASGR1* (Hs01005024_m1), *ASGR2* (Hs00910100_m1), *AFP* (Hs01040598_m1), *AAT* (Hs00165475_m1), and *Lgr6* (Hs00663887_m1). Probe context sequences are available in [Table S1](#).

Housekeeper genes included *PPIB* (peptidylprolyl isomerase B) (Hs00168719_m1) and *B2M* (beta-2 microglobulin) (Hs00984230_m1).

Immunofluorescence

For immunofluorescence staining, organoids embedded in matrigel were washed with phosphate-buffered saline (PBS) (–/–), and

organoids were fixed in 4% paraformaldehyde (Thermo Fisher Scientific, J19943.K2) for 1 h at 4°C. After washing with PBS (–/–) twice, organoids were permeabilized with 0.2% (v/v) Triton X-100 (Sigma, 9036-19-5) in PBS (–/–) for 1 h at RT. Samples were washed twice with PBS (–/–). Subsequently, organoids were incubated with a blocking buffer consisting of 10% (v/v) donkey serum (Sigma, D9663) and 0.01% (v/v) Triton X-100 in PBS (–/–) for 4 h at RT. Samples were washed twice with PBS (–/–). Primary antibodies were diluted in blocking buffer and incubated on the samples at 4°C overnight. Organoids were stained for albumin (Cedarlane Laboratories, CL2513A, 1:100), ASGR1 (Bio-Techne AG, MAB4394-100, 1:50), and alpha 1-antitrypsin (R&D Systems, MAB1268-100, 1:100).

On the next day, organoids were washed twice with PBS (–/–) and incubated with the secondary antibody AF488-donkey-anti-mouse (Thermo Fisher Scientific, A-21202, 1:500) in PBS (–/–) for 1 h at RT protected from light. Samples were washed twice with PBS (–/–). Hoechst 33342 (Invitrogen, H3570) was added and incubated for 10 min at RT protected from light. Samples were washed twice with PBS (–/–) and imaged using the Opera Phenix high-content screening system (PerkinElmer).

Aspartate aminotransferase measurements

AST activity in the supernatant of the culture was analyzed with the Cobas pure c 303 analyzer (Roche Diagnostics International Ltd., Rotkreuz, Switzerland). The measurement range for AST assay with pyridoxal phosphate activation is 5–700 U/L.

Adenosine triphosphate measurements

ATP measurement was performed using the CellTiter-Glo 3D Cell Viability Assay (Promega, G9681) according to manufacturer's instructions.

Image analysis

Image analysis following transduction of GFP-labeled AAVs was carried out using the Incucyte Live-Cell Analysis System (Sartorius).

Image analysis following transduction of GFP-labeled AAVs was carried out using the Harmony High-Content Imaging and Analysis Software (Revvity) and ImageJS to count the number of GFP-positive organoids and the total number of organoids, respectively.

DATA AVAILABILITY

The data that support the key findings of this study are available within the article and supplemental material or upon request from the corresponding author, Estelle Berreur.

ACKNOWLEDGMENTS

This work was funded by Roche Pharma R&D. The graphical abstract was done on BioRender.

AUTHOR CONTRIBUTIONS

E.B., G.L., C.R., and R.M. designed the experiments; E.B., G.L., and C.R. established the model; E.B. performed the experiments; M.Z. and M.S. did the AST measurements; E.B. analyzed the data, made the figures, and wrote the manuscript; R.X., E.B.-N., R.M., and A.B.R. reviewed the manuscript.

DECLARATION OF INTERESTS

All authors are employees of Hoffmann-La Roche. The company provided support in the form of salaries for authors but did not have any additional role in the study design, data collection and analysis, decision to publish, or preparation of the manuscript. During the preparation of this work, the authors used RocheChat in order to improve sentence construction and refine language. After using this tool, the authors reviewed and edited the content as needed and take full responsibility for the content of the publication.

SUPPLEMENTAL INFORMATION

Supplemental information can be found online at <https://doi.org/10.1016/j.omtm.2025.101467>.

REFERENCES

- Athanasopoulos, T., Munye, M.M., and Yáñez-Muñoz, R.J. (2017). Nonintegrating Gene Therapy Vectors. *Hematol. Oncol. Clin. N. Am.* 31, 753–770. <https://doi.org/10.1016/j.hoc.2017.06.007>.
- Russell, S., Bennett, J., Wellman, J.A., Chung, D.C., Yu, Z.-F., Tillman, A., Wittes, J., Pappas, J., Elci, O., McCague, S., et al. (2017). Efficacy and safety of voretigene neparvovec (AAV2-hRPE65v2) in patients with RPE65-mediated inherited retinal dystrophy: a randomised, controlled, open-label, phase 3 trial. *Lancet* 390, 849–860. [https://doi.org/10.1016/S0140-6736\(17\)31868-8](https://doi.org/10.1016/S0140-6736(17)31868-8).
- Mendell, J.R., Al-Zaidy, S., Shell, R., Arnold, W.D., Rodino-Klapac, L.R., Prior, T.W., Lowes, L., Alfano, L., Berry, K., Church, K., et al. (2017). Single-Dose Gene-Replacement Therapy for Spinal Muscular Atrophy. *N. Engl. J. Med.* 377, 1713–1722. <https://doi.org/10.1056/NEJMoa1706198>.
- Heo, Y.-A. (2023). Etranacogene Dezaparvovec: First Approval. *Drugs* 83, 347–352. <https://doi.org/10.1007/s40265-023-01845-0>.
- Hoy, S.M. (2023). Delandistrogene Moxeparvovec: First Approval. *Drugs* 83, 1323–1329. <https://doi.org/10.1007/s40265-023-01929-x>.
- Philippidis, A. (2023). BioMarin's ROCTAVIAN Wins Food and Drug Administration Approval As First Gene Therapy for Severe Hemophilia A. *Hum. Gene Ther.* 34, 665–668. <https://doi.org/10.1089/hum.2023.29251.bfs>.
- Keam, S.J. (2022). Eladocogene Exuparvovec: First Approval. *Drugs* 82, 1427–1432. <https://doi.org/10.1007/s40265-022-01775-3>.
- Dhillon, S. (2024). Fidanacogene Elaparvovec: First Approval. *Drugs* 84, 479–486. <https://doi.org/10.1007/s40265-024-02017-4>.
- GTCT (FMS19). <https://a873679.fmphost.com/fmi/webd/GTCT>.
- Kattenhorn, L.M., Tipper, C.H., Stoica, L., Geraghty, D.S., Wright, T.L., Clark, K.R., and Wadsworth, S.C. (2016). Adeno-Associated Virus Gene Therapy for Liver Disease. *Hum. Gene Ther.* 27, 947–961. <https://doi.org/10.1089/hum.2016.160>.
- Trefts, E., Gannon, M., and Wasserman, D.H. (2017). The liver. *Curr. Biol.* 27, R1147–R1151. <https://doi.org/10.1016/j.cub.2017.09.019>.
- Snyder, R.O., Miao, C.H., Patijn, G.A., Spratt, S.K., Danos, O., Nagy, D., Gown, A. M., Winther, B., Meuse, L., Cohen, L.K., et al. (1997). Persistent and therapeutic concentrations of human factor IX in mice after hepatic gene transfer of recombinant AAV vectors. *Nat. Genet.* 16, 270–276. <https://doi.org/10.1038/ng0797-270>.
- Nathwani, A.C., Reiss, U.M., Tuddenham, E.G.D., Rosales, C., Chowdhary, P., McIntosh, J., Della Peruta, M., Lheriteau, E., Patel, N., Raj, D., et al. (2014). Long-Term Safety and Efficacy of Factor IX Gene Therapy in Hemophilia B. *N. Engl. J. Med.* 371, 1994–2004. <https://doi.org/10.1056/NEJMoa1407309>.
- Manno, C.S., Pierce, G.F., Arruda, V.R., Glader, B., Ragni, M., Rasko, J.J., Ozelo, M. C., Hoots, K., Blatt, P., Konkle, B., et al. (2006). Successful transduction of liver in hemophilia by AAV-Factor IX and limitations imposed by the host immune response. *Nat. Med.* 12, 342–347. <https://doi.org/10.1038/nm1358>.
- Mingozi, F., Maus, M.V., Hui, D.J., Sabatino, D.E., Murphy, S.L., Rasko, J.E.J., Ragni, M.V., Manno, C.S., Sommer, J., Jiang, H., et al. (2007). CD8+ T-cell responses to adeno-associated virus capsid in humans. *Nat. Med.* 13, 419–422. <https://doi.org/10.1038/nm1549>.
- Hinderer, C., Katz, N., Buza, E.L., Dyer, C., Goode, T., Bell, P., Richman, L.K., and Wilson, J.M. (2018). Severe Toxicity in Nonhuman Primates and Piglets Following High-Dose Intravenous Administration of an Adeno-Associated Virus Vector

- Expressing Human SMN. *Hum. Gene Ther.* 29, 285–298. <https://doi.org/10.1089/hum.2018.015>.
17. Huichalaf, C., Perfitt, T.L., Kuperman, A., Gooch, R., Kovi, R.C., Brennehan, K.A., Chen, X., Hirehallur-Shanthappa, D., Ma, T., Assaf, B.T., et al. (2022). In vivo over-expression of frataxin causes toxicity mediated by iron-sulfur cluster deficiency. *Mol. Ther. Methods Clin. Dev.* 24, 367–378. <https://doi.org/10.1016/j.omtm.2022.02.002>.
 18. Palazzi, X., Pardo, I.D., Sirivelu, M.P., Newman, L., Kumpf, S.W., Qian, J., Franks, T., Lopes, S., Liu, J., Monarski, L., et al. (2022). Biodistribution and Tolerability of AAV-PHP.B-CBh-SMN1 in Wistar Han Rats and Cynomolgus Macaques Reveal Different Toxicologic Profiles. *Hum. Gene Ther.* 33, 175–187. <https://doi.org/10.1089/hum.2021.116>.
 19. Suh, D.A., Kao, S.-C., Mao, T., Whiteley, L., Denise, H., Souberbielle, B., Burdick, A. D., Hayes, K., Wright, J.F., Lavender, H., et al. (2012). Safe, Long-term Hepatic Expression of Anti-HCV shRNA in a Nonhuman Primate Model. *Mol. Ther.* 20, 1737–1749. <https://doi.org/10.1038/mt.2012.119>.
 20. Nathwani, A.C., Rosales, C., McIntosh, J., Rastegarlar, G., Nathwani, D., Raj, D., Nawathe, S., Waddington, S.N., Bronson, R., Jackson, S., et al. (2011). Long-term Safety and Efficacy Following Systemic Administration of a Self-complementary AAV Vector Encoding Human FIX Pseudotyped With Serotype 5 and 8 Capsid Proteins. *Mol. Ther.* 19, 876–885. <https://doi.org/10.1038/mt.2010.274>.
 21. Nathwani, A.C., Tuddenham, E.G.D., Rangarajan, S., Rosales, C., McIntosh, J., Linch, D.C., Chowdhary, P., Riddell, A., Pie, A.J., Harrington, C., et al. (2011). Adenovirus-Associated Virus Vector-Mediated Gene Transfer in Hemophilia B. *N. Engl. J. Med.* 365, 2357–2365. <https://doi.org/10.1056/NEJMoa1108046>.
 22. Davidoff, A.M., Gray, J.T., Ng, C.Y.C., Zhang, Y., Zhou, J., Spence, Y., Bakar, Y., and Nathwani, A.C. (2005). Comparison of the ability of adeno-associated viral vectors pseudotyped with serotype 2, 5, and 8 capsid proteins to mediate efficient transduction of the liver in murine and nonhuman primate models. *Mol. Ther.* 11, 875–888. <https://doi.org/10.1016/j.yimthe.2004.12.022>.
 23. Maestro, S., Weber, N.D., Zabaleta, N., Aldabe, R., and Gonzalez-Aseguinolaza, G. (2021). Novel vectors and approaches for gene therapy in liver diseases. *JHEP Rep.* 3, 100300. <https://doi.org/10.1016/j.jhepr.2021.100300>.
 24. Lisowski, L., Dane, A.P., Chu, K., Zhang, Y., Cunningham, S.C., Wilson, E.M., Nygaard, S., Grompe, M., Alexander, I.E., and Kay, M.A. (2014). Selection and evaluation of clinically relevant AAV variants in a xenograft liver model. *Nature* 506, 382–386. <https://doi.org/10.1038/nature12875>.
 25. Liu, S., Razon, L., Ritchie, O., Sih, C.-R., Handyside, B., Berguig, G., Woloszynek, J., Zhang, L., Batty, P., Lillicrap, D., et al. (2022). Application of in-vitro-cultured primary hepatocytes to evaluate species translatability and AAV transduction mechanisms of action. *Mol. Ther. Methods Clin. Dev.* 26, 61–71. <https://doi.org/10.1016/j.omtm.2022.05.008>.
 26. Li, H., Lasaro, M.O., Jia, B., Lin, S.W., Haut, L.H., High, K.A., and Ertl, H.C.J. (2011). Capsid-specific T-cell Responses to Natural Infections With Adeno-associated Viruses in Humans Differ From Those of Nonhuman Primates. *Mol. Ther.* 19, 2021–2030. <https://doi.org/10.1038/mt.2011.81>.
 27. Chandra, S., Long, B.R., Fonck, C., Melton, A.C., Arens, J., Woloszynek, J., and O'Neill, C.A. (2023). Safety Findings of Dosing Gene Therapy Vectors in NHP With Pre-existing or Treatment-Emergent Anti-capsid Antibodies. *Toxicol. Pathol.* 51, 246–256. <https://doi.org/10.1177/01926233231202995>.
 28. Shayakhmetov, D.M., Li, Z.-Y., Ni, S., and Lieber, A. (2004). Analysis of Adenovirus Sequestration in the Liver, Transduction of Hepatic Cells, and Innate Toxicity after Injection of Fiber-Modified Vectors. *J. Virol.* 78, 5368–5381. <https://doi.org/10.1128/jvi.78.10.5368-5381.2004>.
 29. Morgan, K., Martucci, N., Kozłowska, A., Gamal, W., Brzeszczyński, F., Treskes, P., Samuel, K., Hayes, P., Nelson, L., Bagnaninchi, P., et al. (2019). Chlorpromazine toxicity is associated with disruption of cell membrane integrity and initiation of a pro-inflammatory response in the HepaRG hepatic cell line. *Biomed. Pharmacother.* 111, 1408–1416. <https://doi.org/10.1016/j.biopha.2019.01.020>.
 30. Anthérieu, S., Bachour-El Azzi, P., Dumont, J., Abdel-Razzak, Z., Guguen-Guillouzo, C., Fromenty, B., Robin, M.A., and Guillouzo, A. (2013). Oxidative stress plays a major role in chlorpromazine-induced cholestasis in human HepaRG cells. *Hepatology* 57, 1518–1529. <https://doi.org/10.1002/hep.26160>.
 31. Zhao, J., Yue, Y., Patel, A., Wasala, L., Karp, J.F., Zhang, K., Duan, D., and Lai, Y. (2020). High-Resolution Histological Landscape of AAV DNA Distribution in Cellular Compartments and Tissues following Local and Systemic Injection. *Mol. Ther. Methods Clin. Dev.* 18, 856–868. <https://doi.org/10.1016/j.omtm.2020.08.006>.
 32. Ellis, B.L., Hirsch, M.L., Barker, J.C., Connelly, J.P., Steininger, R.J., and Porteus, M. H. (2013). A survey of ex vivo/in vitro transduction efficiency of mammalian primary cells and cell lines with Nine natural adeno-associated virus (AAV1-9) and one engineered adeno-associated virus serotype. *Virol. J.* 10, 74. <https://doi.org/10.1186/1743-422X-10-74>.
 33. Pillay, S., Meyer, N.L., Puschnik, A.S., Davulcu, O., Diep, J., Ishikawa, Y., Jae, L.T., Wosen, J.E., Nagamine, C.M., Chapman, M.S., and Carette, J.E. (2016). An essential receptor for adeno-associated virus infection. *Nature* 530, 108–112. <https://doi.org/10.1038/nature16465>.
 34. Summerford, C., and Samulski, R.J. (1998). Membrane-Associated Heparan Sulfate Proteoglycan Is a Receptor for Adeno-Associated Virus Type 2 Virions. *J. Virol.* 72, 1438–1445. <https://doi.org/10.1128/JVI.72.2.1438-1445.1998>.
 35. Wu, Z., Miller, E., Agbandje-McKenna, M., and Samulski, R.J. (2006). $\alpha 2,3$ and $\alpha 2,6$ N-Linked Sialic Acids Facilitate Efficient Binding and Transduction by Adeno-Associated Virus Types 1 and 6. *J. Virol.* 80, 9093–9103. <https://doi.org/10.1128/JVI.00895-06>.
 36. Akache, B., Grimm, D., Shen, X., Fuess, S., Yant, S.R., Glazer, D.S., Park, J., and Kay, M.A. (2007). A Two-hybrid Screen Identifies Cathepsins B and L as Uncoating Factors for Adeno-associated Virus 2 and 8. *Mol. Ther.* 15, 330–339. <https://doi.org/10.1038/sj.mt.6300053>.
 37. Qing, K., Mah, C., Hansen, J., Zhou, S., Dwarki, V., and Srivastava, A. (1999). Human fibroblast growth factor receptor 1 is a co-receptor for infection by adeno-associated virus 2. *Nat. Med.* 5, 71–77. <https://doi.org/10.1038/4758>.
 38. Weller, M.L., Amornphimoltham, P., Schmidt, M., Wilson, P.A., Gutkind, J.S., and Chiorini, J.A. (2010). Epidermal growth factor receptor is a co-receptor for adeno-associated virus serotype 6. *Nat. Med.* 16, 662–664. <https://doi.org/10.1038/nm.2145>.
 39. Baruteau, J., Brunetti-Pierri, N., and Gissen, P. (2024). Liver-directed gene therapy for inherited metabolic diseases. *J. Inher. Metab. Dis.* 47, 9–21. <https://doi.org/10.1002/jimd.12709>.
 40. Dixon, L.J., Barnes, M., Tang, H., Pritchard, M.T., and Nagy, L.E. (2013). Kupffer cells in the liver. *Compr. Physiol.* 3, 785–797. <https://doi.org/10.1002/cphy.c120026>.